



Heavy metal pollution of coal mine-affected agricultural soils in the northern part of Bangladesh

Mohammad A.H. Bhuiyan^{a,b,*}, Lutfar Parvez^b, M.A. Islam^c, Samuel B. Dampare^d, Shigeyuki Suzuki^a

^a Graduate School of Natural Science & Technology, Okayama University, Okayama 700-8530, Japan

^b Department of Environmental Sciences, Jahangirnagar University, Dhaka 1342, Bangladesh

^c Chemistry Division, Atomic Energy Center, Dhaka, Bangladesh

^d National Nuclear Research Institute, Ghana Atomic Energy Commission, P.O. Box LG 80, Legon, Accra, Ghana

ARTICLE INFO

Article history:

Received 18 June 2009

Received in revised form 15 August 2009

Accepted 19 August 2009

Available online 25 August 2009

Keywords:

Enrichment

Geoaccumulation

Pollution load index

Heavy metals

Principal component

Mine drainage

ABSTRACT

Total concentrations of heavy metals in the soils of mine drainage and surrounding agricultural fields in the northern part of Bangladesh were determined to evaluate the level of contamination. The average concentrations of Ti, Mn, Zn, Pb, As, Fe, Rb, Sr, Nb and Zr exceeded the world normal averages and, in some cases, Mn, Zn, As and Pb exceeded the toxic limit of the respective metals. Soil pollution assessment was carried out using enrichment factor (EF), geoaccumulation index (I_{geo}) and pollution load index (PLI). The soils show significant enrichment with Ti, Mn, Zn, Pb, As, Fe, Sr and Nb, indicating inputs from mining activities. The I_{geo} values have revealed that Mn (1.24 ± 0.38), Zn (1.49 ± 0.58) and Pb (1.63 ± 0.38) are significantly accumulated in the study area. The PLIs derived from contamination factors indicate that the distal part of the coal mine-affected area is the most polluted (PLI of 4.02). Multivariate statistical analyses, principal component and cluster analyses, suggest that Mn, Zn, Pb and Ti are derived from anthropogenic sources, particularly coal mining activities, and the extreme proximal and distal parts are heavily contaminated with maximum heavy metals.

© 2009 Elsevier B.V. All rights reserved.

1. Introduction

Coal plays an important role in energy generation, and approximately 27% of the world's energy consumption originates from the incineration of coal. Underground and open pit coal exploitation includes a phase development in mine and removal of surrounding rocks, which are low in coal content (<30%) and often contain iron sulfide minerals. During the process of opencast and underground coal mining, a variety of rock types with different compositions are exposed to atmospheric conditions and undergo accelerated weathering. These materials are often deposited nearby as mine waste rocks and mine dust.

Acid mine drainage (AMD), which usually occurs at coal mining sites in the world, represents serious environmental problems for the global community. AMD can occur during the exploitation of coal and coal-bearing minerals, and ore bodies containing acid-forming metal sulfides such as pyrite (FeS_2) [1]. The oxidation of such sulfides exposed to atmospheric O_2 during or after mining activities generates acidic waters with high dissolved SO_4^{2-} , Fe,

and heavy metals. The low pH may cause further dissolution of local country rock and leaching of additional metals into water [2], thereby adversely impacting on aquatic life and the surrounding vegetation [3].

Earlier studies on environmental impacts of coal mining have shown that soil acidity, toxic metal concentrations [4] and vegetation damage [5] are the predominant negative impacts of AMD. Seepage of water from overburden dumps, exposed overburden and coal processing etc. constitutes mining effluent, which contains heavy metals [6]. Pollution of the natural environment by heavy metals is a worldwide problem because these metals are indestructible and most of them have toxic effects on living organisms at certain concentrations [7].

The Barapukuria coal mine, located in the northern part of Bangladesh, has the potential of contributing significantly to resolving the current energy crisis and improving the living standards in Bangladesh. It will bring long term social and economic benefits to the country. However, the cumulative effects of exploration activities at multiple sites within an area have the potential to drive environmental change, particularly from a larger regional perspective. The more common and noticeable effects of these cumulative impacts include changes in aquatic and terrestrial ecosystem health. In order to take the initiative for remediation of affected soil, necessary information is required on the extent of pollution. This work is, therefore, carried out to explore the degree

* Corresponding author at: Graduate School of Natural Science & Technology, Okayama University, Okayama 700-8530, Japan. Tel.: +81 86 251 7881; fax: +81 86 251 7895.

E-mail address: amirhb75@yahoo.com (M.A.H. Bhuiyan).

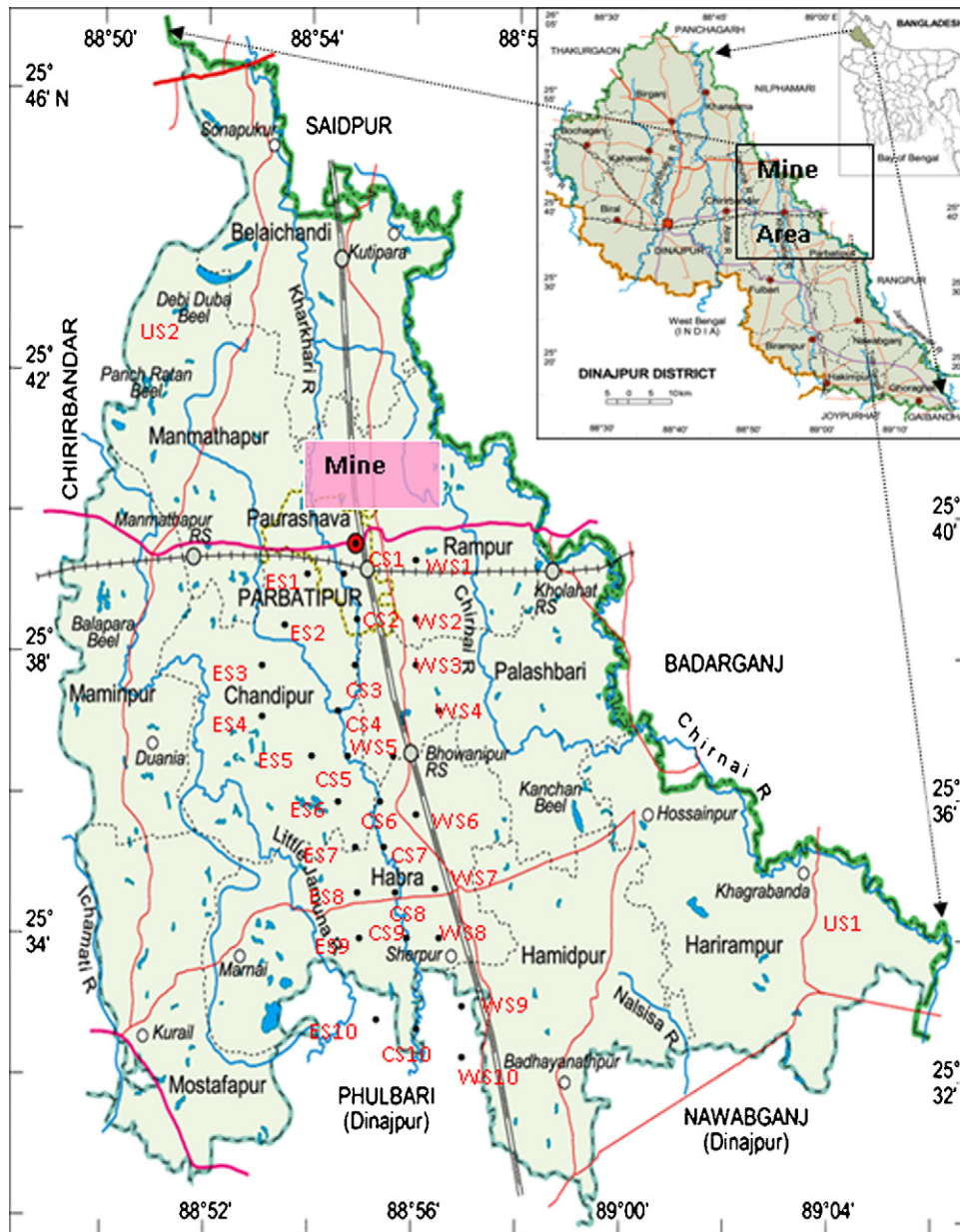


Fig. 1. Location map of the study area.

and spatial distribution of heavy metal pollution of the coal mine-affected agricultural soils in northern Bangladesh.

2. Study area

Barapukuria coal basin is located in Dinajpur District of northern part of Bangladesh. It lies between latitudes $25^{\circ}31'45''\text{N}$ and $25^{\circ}33'5''\text{N}$, and longitudes $88^{\circ}57'48''\text{E}$ and $88^{\circ}58'53''\text{E}$ (Fig. 1). The two big rivers, Ganges and Brahmaputra, separate the northwestern part of Bangladesh from the other parts. The main drainage system of the study area includes Atrai, Little Jamuna, Karatoa, Bandali. All the rivers originate from the Himalayas in the north and flow towards south and southeast. A few small rivers have cut across the Pleistocene Barind Tract towards the south, while the others flow along the eastern and western margins of the upland. Maddhapara and its adjoining areas are part of the Barind Tract, which is drained by local Jamuna river in the west and Jabuneswari river in the east. The Kala river, an intermittent stream and a distributary of the Chir-

nai river (Fig. 1), is separated from Chirnai at Kasamat Union and rejoins Chirnai at Debipur union.

3. Methodology

3.1. Sample collection

Thirty-two surface soil samples (from 5 to 15 cm depth), consisting of 10 from mine drainage (samples prefixed CS) and 20 from agriculture field, were collected in polyethylene bags with a stainless spatula. Of the agricultural soils, 10 samples each were collected from the west bank (prefixed WS) and east bank (prefixed ES) of the irrigation drainage. The 30 sampling points were classified into 10 sampling sites as follows: Site 1 (ES1, WS1, CS1), Site 2 (ES2, WS2, CS2), Site 3 (ES3, WS3, CS3), Site 4 (ES4, WS4, CS4), Site 5 (ES5, WS5, CS5), Site 6 (ES6, WS6, CS6), Site 7 (ES7, WS7, CS7), Site 8 (ES8, WS8, CS8), Site 9 (ES9, WS9, CS9) and Site 10 (ES10, WS10, CS10). The sampling points were separated linearly by 50 m and

laterally by approximately 20 m (Fig. 1). Two unaffected soil samples (US1 and US2) were also collected from an agricultural land at a distance of about 7 km from the coal mine influenced area for background studies.

3.2. Measurement of physico-chemical properties

The pH and EC of the samples were measured with a JENWAY pH meter (Model 3051) and JENWAY conductivity meter (Model 4070) calibrated with a buffer solution (pH 7), respectively. The total organic carbon content (TOC) in soil samples was measured by titration method, using FeSO_4 after digestion of samples with $\text{K}_2\text{Cr}_2\text{O}_7\text{--H}_2\text{SO}_4$ solution [8].

3.3. Elemental analysis by EDXRF method

The elemental analysis was performed by energy dispersive X-ray fluorescence (EDXRF) spectrometer at the Chemistry Division of Atomic Energy Centre, Dhaka. The experimental setup and the data acquisition system consist of a Cd-109 radioisotope annular source (NEN), a Si (Li) detector (Canberra, Model SL 80175), a fast spectroscopy amplifier (Canberra, Model 2024), a high voltage power supply (Tennelec, Model TC 950A), and a multi channel analyzer (Canberra, Series 35, Model 3201). The detection limits of elements in the samples were calculated from the experimental background counts and were plotted as a function of their atomic numbers [9]. The minimum detection limits (in mg/kg) of heavy metals in the studied soils are: 1204 (K), 915 (Ca), 116 (Ti), 86 (Mn), 65 (Fe), 12 (Zn), 20 (Pb), 5.28 (Rb), 7.5 (Sr), 20 (Zr) and 15 (Nb) in XRF analytical methods. The detection limit of As has been measured as 0.001 mg/kg in AAS methods. The analytical precision and accuracy on the XRF technique was accomplished by analyzing six replicate samples of IAEA certified material, Soil-7. The precision was better than 10% for all analyzed elements. XRF-data processing and the quantitative analysis were performed using software called quantitative X-ray analysis system (QXAS) [10]. The peak integration and all necessary corrections were made by QXAS through optimization of all parameters. Arsenic was measured by a PerkinElmer Atomic Absorption Spectrophotometer (Model 3110).

3.4. Quantification of soil pollution

3.4.1. Enrichment factors (EF)

The enrichment factor for each metal is calculated by dividing its ratio to the normalizing element by the same ratio found in the chosen baseline [11]. Thus, EF is computed using the relationship below:

$$EF = \frac{(\text{Metal/Fe})_{\text{Sample}}}{(\text{Metal/Fe})_{\text{Background}}}$$

Rubio et al. [12] recommended the use of regional background values. While the geochemical background values are constant, the levels of contamination vary with time and places. Background values are distinctly different among different soil types, especially with respect to Na, Mg, Al, K, Ca, Ba, Sc, Ti, Fe and Br [13]. For most heavy metals of environmental interest, concentrations in soil easily vary over 2–3 orders of magnitude depending on the parent materials [14]. In this regard, the background values in the present study were calculated from the mean concentrations of heavy metals in unaffected soils of the study area, following the approach of Cabrera et al. [15] and Yaqin et al. [16]. The EF values close to unity indicate crusted origin, those less than 1.0 suggest a possible mobilization or depletion of metals [17], whereas $EF > 1.0$ indicates that the element is of anthropogenic origin. EFs greater than 10 are considered to be non-crusted source. In this study, iron (Fe) was used

as the reference element for geochemical normalization because of the following reasons: (1) Fe is associated with fine solid surfaces; (2) its geochemistry is similar to that of many trace metals and (3) its natural concentration tends to be uniform [18].

3.4.2. Geoaccumulation index (I_{geo})

Geoaccumulation indexes for the metals were determined using Muller's [19] expression:

$$I_{geo} = \frac{\text{Log}_2(C_n)}{1.5(B_n)}$$

where C_n is the concentration of metals examined in soil samples and B_n is the geochemical background concentration of the metal (n). Factor 1.5 is the background matrix correction factor due to lithospheric effects. The geoaccumulation index consists of seven grades or classes [20]. Class 0 (practically uncontaminated): $I_{geo} \leq 0$; Class 1 (uncontaminated to moderately contaminated): $0 < I_{geo} < 1$; Class 2 (moderately contaminated): $1 < I_{geo} < 2$; Class 3 (moderately to heavily contaminated): $2 < I_{geo} < 3$; Class 4 (heavily contaminated): $3 < I_{geo} < 4$; Class 5 (heavily to extremely contaminated): $4 < I_{geo} < 5$; Class 6 (extremely contaminated): $5 < I_{geo}$. Class 6 is an open class and comprises all values of the index higher than Class 5. The elemental concentrations in Class 6 may be hundredfold greater than the geochemical background value.

3.4.3. Contamination factor (CF)

The CF is the ratio obtained by dividing the concentration of each metal in the soil by the baseline or background value (concentration in unpolluted soil):

$$CF = \frac{C_{\text{heavy metal}}}{C_{\text{background}}}$$

The contamination levels may be classified based on their intensities on a scale ranging from 1 to 6 (0 = none, 1 = none to medium, 2 = moderate, 3 = moderately to strong, 4 = strongly polluted, 5 = strong to very strong, 6 = very strong) [21]. The highest number indicates that the metal concentration is 100 times greater than what would be expected in the crust.

3.4.4. Pollution load index (PLI)

For the entire sampling site, PLI has been determined as the n th root of the product of the n CF [22]:

$$PLI = (CF_1 \times CF_2 \times CF_3 \times \dots \times CF_n)^{1/n}$$

This empirical index provides a simple, comparative means for assessing the level of heavy metal pollution.

3.5. Statistical analysis

The experimental data were treated statistically using SPSS software (version 17.0 for Windows). Principal component analysis (PCA) was employed to infer the hypothetical source of heavy metals (natural or anthropogenic). Factor analysis (FA), the components of the PCA was performed by Varimax rotation. Varimax rotation was employed because orthogonal rotation minimizes the number of variables with a high loading on each component and therefore facilitates the interpretation of PCA results. Cluster analysis (CA) was applied to identify different geochemical groups, clustering the samples with similar heavy metal contents. CA was formulated according to the Ward-algorithmic method, and the squared Euclidean distance was employed for measuring the distance between clusters of similar metal contents. Pearson's product moment correlation matrix was used to identify the relationship among metals and support the results obtained by multivariate analysis.

Table 1
Descriptive statistics, enrichment factors and geoaccumulation indices (I_{geo}) of heavy metals for agricultural soil.

Sample	pH	EC ($\mu\text{S m}^{-1}$)	TOC (mg/kg)	K			Ca			Ti			Mn			Fe			Zn		
				Concentration (mg/kg)	EF	I_{geo}	Concentration (mg/kg)	EF	I_{geo}	Concentration (mg/kg)	EF	I_{geo}	Concentration (mg/kg)	EF	I_{geo}	Concentration (mg/kg)	EF	I_{geo}	Concentration (mg/kg)	EF	I_{geo}
				ES1	6.73	43	55.54	11000 ± 300	1.49	0.56	77000 ± 600	16.01	3.98	14600 ± 100	1.96	0.95	2219 ± 11	2.92	1.53	51300 ± 200	2.92
ES2	6.58	82	15.18	10500 ± 1500	1.61	0.49	28700 ± 700	6.74	2.56	10800 ± 100	1.64	0.52	2204 ± 23	3.27	1.52	45400 ± 100	1.00	(0.20)	255 ± 10	3.00	1.39
ES3	7.88	190	14.01	12600 ± 300	2.01	0.75	17000 ± 100	4.17	1.80	12700 ± 200	2.01	0.75	1289 ± 13	2.00	0.74	43500 ± 100	1.00	(0.26)	219 ± 11	2.69	1.17
ES4	8.70	190	15.69	10400 ± 500	1.99	0.47	16500 ± 800	4.85	1.76	11300 ± 300	2.14	0.58	1943 ± 24	3.61	1.33	36300 ± 700	1.00	(0.52)	443 ± 12	6.53	2.19
ES5	7.70	195	22.25	12200 ± 400	1.19	0.70	12600 ± 400	1.90	1.37	18700 ± 800	1.82	1.31	1642 ± 12	1.56	1.09	70900 ± 500	1.00	0.45	362 ± 19	2.73	1.90
ES6	6.25	41	6.79	21400 ± 700	1.91	1.52	52200 ± 600	7.14	3.42	13700 ± 300	1.21	0.86	1442 ± 19	1.25	0.90	78000 ± 200	1.00	0.59	129 ± 9	0.88	0.41
ES7	7.79	209	23.35	22400 ± 600	3.71	1.58	42800 ± 100	10.89	3.13	12500 ± 100	2.05	0.73	1204 ± 12	1.94	0.64	41900 ± 900	1.00	(0.31)	144 ± 12	1.84	0.57
ES8	7.78	160	27.36	11500 ± 700	1.10	0.62	32800 ± 100	4.83	2.75	17200 ± 300	1.64	1.19	3154 ± 25	2.94	2.03	72400 ± 200	1.00	0.48	460 ± 19	3.40	2.24
ES9	7.77	185	14.94	11400 ± 200	1.11	0.61	22800 ± 200	3.41	2.23	11000 ± 400	1.06	0.54	1620 ± 16	1.53	1.07	71300 ± 800	1.00	0.46	163 ± 7	1.22	0.75
ES10	7.75	175	16.22	12200 ± 300	1.36	0.70	20800 ± 100	3.56	2.09	12000 ± 100	1.33	0.67	1856 ± 18	2.01	1.27	62300 ± 100	1.00	0.26	143 ± 5	1.23	0.56
WS1	6.50	83	45.54	16300 ± 130	2.39	1.12	66800 ± 500	15.06	3.78	15600 ± 400	2.27	1.05	2099 ± 15	2.99	1.44	47300 ± 300	1.00	(0.14)	416 ± 12	4.70	2.10
WS2	6.70	76	21.18	21100 ± 500	2.91	1.49	26100 ± 300	5.52	2.42	12800 ± 100	1.75	0.76	2112 ± 28	2.83	1.45	50400 ± 200	1.00	(0.04)	273 ± 11	2.90	1.49
WS3	7.30	160	15.12	15100 ± 100	2.26	1.01	16000 ± 700	3.67	1.71	10700 ± 300	1.58	0.50	1485 ± 15	2.15	0.95	46500 ± 400	1.00	(0.16)	279 ± 10	3.21	1.52
WS4	6.70	182	14.19	13400 ± 700	2.37	0.84	17100 ± 200	4.65	1.81	12500 ± 100	2.20	0.73	2133 ± 25	3.67	1.47	39200 ± 100	1.00	(0.41)	455 ± 42	6.21	2.23
WS5	7.00	191	12.55	15200 ± 130	1.51	1.02	13200 ± 200	2.01	1.44	17700 ± 500	1.74	1.23	1589 ± 22	1.53	1.04	69900 ± 500	1.00	0.43	402 ± 16	3.08	2.05
WS6	6.50	121	16.38	20400 ± 200	1.94	1.45	49600 ± 300	7.26	3.35	13500 ± 200	1.28	0.84	1456 ± 32	1.35	0.92	72900 ± 400	1.00	0.49	239 ± 17	1.75	1.30
WS7	7.76	189	20.05	19400 ± 800	2.96	1.37	48800 ± 400	11.44	3.32	15600 ± 300	2.36	1.05	1194 ± 27	1.77	0.63	45500 ± 800	1.00	(0.19)	154 ± 7	1.81	0.66
WS8	8.00	142	29.46	16500 ± 700	1.54	1.14	29800 ± 700	4.27	2.61	18100 ± 100	1.68	1.26	2883 ± 24	2.61	1.90	74400 ± 200	1.00	0.52	163 ± 7	3.38	2.27
WS9	7.78	173	24.94	22500 ± 200	2.25	1.59	23600 ± 200	3.63	2.28	11900 ± 700	1.18	0.66	1830 ± 18	1.78	1.25	69300 ± 100	1.00	0.41	216 ± 14	1.67	1.15
WS10	8.20	169	19.11	21700 ± 100	2.06	1.54	18000 ± 100	2.62	1.88	10900 ± 200	1.02	0.53	2025 ± 13	1.86	1.39	73300 ± 900	1.00	0.50	196 ± 9	1.43	1.01
CS1	6.13	85	64.14	20100 ± 200	2.20	1.42	54400 ± 600	9.15	3.48	17600 ± 600	1.91	1.22	2311 ± 17	2.46	1.58	63400 ± 100	1.00	0.29	432 ± 13	3.64	2.15
CS2	6.50	96	51.21	19510 ± 500	2.06	1.38	47700 ± 100	7.73	3.29	11700 ± 300	1.22	0.63	2244 ± 30	2.30	1.54	65800 ± 400	1.00	0.34	305 ± 11	2.48	1.65
CS3	6.88	180	44.11	21600 ± 400	3.70	1.53	21200 ± 400	5.58	2.12	17700 ± 400	3.01	1.23	1438 ± 15	2.39	0.90	40500 ± 700	1.00	(0.36)	279 ± 7	3.68	1.52
CS4	7.00	200	25.19	18400 ± 100	2.31	1.30	19500 ± 800	3.76	2.00	13100 ± 100	1.63	0.79	1844 ± 23	2.25	1.26	55300 ± 100	1.00	0.09	356 ± 14	3.44	1.87
CS5	6.80	185	27.55	17200 ± 500	1.62	1.20	36600 ± 500	5.28	2.91	19700 ± 800	1.84	1.38	1522 ± 12	1.39	0.98	73900 ± 500	1.00	0.51	422 ± 12	3.05	2.12
CS6	6.75	94	18.72	20400 ± 200	2.06	1.45	47200 ± 400	7.31	3.28	15700 ± 700	1.57	1.06	1402 ± 11	1.37	0.86	68900 ± 200	1.00	0.41	218 ± 7	1.69	1.17
CS7	8.00	210	33.45	21400 ± 100	2.76	1.52	40800 ± 300	8.07	3.07	15400 ± 400	1.97	1.03	1314 ± 14	1.64	0.77	53900 ± 900	1.00	0.05	185 ± 14	1.83	0.92
CS8	8.20	198	37.16	19500 ± 700	1.80	1.38	52400 ± 200	7.41	3.43	17900 ± 500	1.63	1.25	3255 ± 11	2.91	2.08	75400 ± 700	1.00	0.54	420 ± 22	2.98	2.11
CS9	6.80	201	54.72	21100 ± 200	2.25	1.49	34800 ± 100	5.70	2.84	11100 ± 400	1.17	0.56	1840 ± 17	1.91	1.25	65100 ± 100	1.00	0.32	244 ± 10	2.00	1.33
CS10	7.00	95	24.44	24400 ± 400	2.37	1.70	18800 ± 400	2.81	1.95	19100 ± 100	1.84	1.34	2020 ± 28	1.91	1.39	71400 ± 300	1.00	0.46	233 ± 11	1.75	1.26
Max	8.70	210	64.14	24400			77000			19700			3255			78000			470		
Min	6.13	41	6.79	10400			12600			10700			1194			36300			129		
SD	0.68	53	14.78	4348			17053			2912			530			13318			111		
Mean	7.25	150	27.02	17360			33520			14427			1886			59853			296		
World normal			15000				24000			2900			550			26000			60		
Toxic limit			15000										1500(3000)						70(400)		

Sample	As			Rb			Sr			Pb			Zr			Nb		
	Concentration (mg/kg)	EF	I_{geo}	Concentration (mg/kg)	EF	I_{geo}	Concentration (mg/kg)	EF	I_{geo}	Concentration (mg/kg)	EF	I_{geo}	Concentration (mg/kg)	EF	I_{geo}	Concentration (mg/kg)	EF	I_{geo}
ES1	8.25 ± 0.02	0.51	-0.98	182 ± 6.0	0.89	-0.19	408 ± 21	7.16	2.82	490 ± 17	3.66	1.85	1150 ± 12	4.86	2.26	70 ± 6.0	4.30	2.08
ES2	10.80 ± 0.01	0.76	-0.59	120 ± 5.0	0.66	-0.79	256 ± 17	5.08	2.15	521 ± 18	4.40	1.94	573 ± 17	2.73	1.26	67 ± 4.0	4.65	2.02
ES3	14.20 ± 0.01	1.04	-0.20	182 ± 5.0	1.05	-0.19	257 ± 10	5.32	2.15	345 ± 12	3.04	1.35	1619 ± 29	8.06	2.75	120 ± 11	8.69	2.86
ES4	17.60 ± 0.01	1.55	0.11	80.4 ± 3.0	0.55	-1.37	315 ± 13	7.81	2.45	373 ± 15	3.94	1.46	526 ± 16	3.14	1.13	55 ± 3.0	4.77	1.74
ES5	9.30 ± 0.05	0.42	-0.81	214 ± 4.0	0.76	0.04	555 ± 33	7.05	3.26	471 ± 36	2.54	1.79	1099 ± 16	3.36	2.20	95 ± 9.0	4.22	2.53
ES6	21.70 ± 0.09	0.89	0.41	308 ± 6.0	0.99	0.57	147 ± 9	1.70	1.35	446 ± 10	2.19	1.72	983 ± 19	2.73	2.03	54 ± 4.0	2.18	1.71
ES7	13.00 ± 0.07	0.99	-0.33	155 ± 4.0	0.93	-0.42	70 ± 5	1.50	0.28	155 ± 8	1.42	0.19	826 ± 17	4.27	1.78	25 ± 1.2	1.88	0.60
ES8	22.70 ± 0.02	1.00	0.48	238 ± 6.0	0.82	0.20	501 ± 30	6.23	3.12	498 ± 13	2.63	1.88	883 ± 12	2.64	1.88	80 ± 6.5	3.48	2.28
ES9	24.40 ± 0.08	1.09	0.58	234 ± 3.0	0.82	0.17	98 ± 6	1.24	0.76	331 ± 13	1.78	1.29	19.5 ± 14	0.06	-3.62	19.9 ± 0.1	0.88	0.27
ES10	19.20 ± 0.02	0.98	0.24	184 ± 4.0	0.74	-0.18	188 ± 8	2.72	1.70	382 ± 17	2.35	1.49	681 ± 11	2.37	1.50	70 ± 6.0	3.54	2.08
WS1	9.64 ± 0.01	0.65	-0.76	211 ± 11	1.12	0.02	368 ± 14	7.00	2.67	445 ± 16	3.60	1.71	1240 ± 22	5.68	2.37	77 ± 5.0	5.13	2.22
WS2	12.60 ± 0.04	0.80	-0.37	98 ± 7.3	0.49	-1.08	306 ± 13	5.47	2.41	519 ± 12	3.94	1.93	633 ± 18	2.72	1.40	96 ± 8.0	6.00	2.54
WS3	13.12 ± 0.01	0.90	-0.31	223 ± 4.1	1.20	0.10	277 ± 15	5.36	2.26	355 ± 19	2.92	1.39	1225 ± 79	5.71	2.35	104 ± 10	7.05	2.66

Table 1 (Continued)

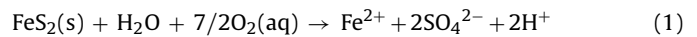
Sample	As			Rb			Sr			Pb			Zr			Nb		
	Concentration (mg/kg)	EF	I _{geo}	Concentration (mg/kg)	EF	I _{geo}	Concentration (mg/kg)	EF	I _{geo}	Concentration (mg/kg)	EF	I _{geo}	Concentration (mg/kg)	EF	I _{geo}	Concentration (mg/kg)	EF	I _{geo}
WS4	20.00±0.02	1.63	0.29	96.2±8.0	0.61	-1.11	415±26	9.53	2.85	423±14	4.13	1.64	556±26	3.07	1.21	115±8.0	9.24	2.80
WS5	19.30±0.01	0.88	0.24	213±3.6	0.76	0.04	455±24	5.86	2.98	441±19	2.42	1.70	1102±48	3.42	2.20	91±6.0	4.10	2.46
WS6	22.20±0.01	0.97	0.44	289±6.2	0.99	0.48	159±9	1.96	1.46	406±18	2.13	1.58	1005±36	2.99	2.07	85±4.5	3.67	2.36
WS7	14.10±0.02	0.99	-0.21	171±6.2	0.94	-0.28	163±15	3.23	1.50	265±17	2.23	0.97	986±25	4.69	2.04	125±10	8.66	2.92
WS8	21.60±0.08	0.93	0.41	242±4.3	0.81	0.22	478±15	5.78	3.05	512±15	2.64	1.92	772±44	2.25	1.69	88±6.2	3.73	2.42
WS9	26.40±0.05	1.21	0.69	224±3.6	0.81	0.11	198±16	2.57	1.78	372±13	2.06	1.45	19.5±0.1	0.06	-3.62	19.9±0.1	0.90	0.27
WS10	22.10±0.09	0.96	0.44	194±6.4	0.66	-0.10	108±7	1.33	0.90	468±14	2.45	1.79	1122±25	3.32	2.22	67±4.1	2.88	2.02
CS1	10.10±0.02	0.51	-0.69	193±8.2	0.76	-0.11	500±35	7.10	3.11	470±22	2.84	1.79	1232±12	4.21	2.36	87±7.2	4.32	2.40
CS2	11.00±0.06	0.53	-0.57	164±9	0.62	-0.34	316±22	4.32	2.45	532±11	3.10	1.97	674±17	2.22	1.49	96±8.5	4.60	2.54
CS3	16.10±0.02	1.27	-0.02	192±10	1.19	-0.11	248±24	5.51	2.10	335±19	3.17	1.30	1822±32	9.75	2.92	99±6.5	7.70	2.58
CS4	22.40±0.01	1.29	0.46	172±9	0.78	-0.27	311±12	5.06	2.43	382±15	2.65	1.49	612±22	2.40	1.35	64±4.4	3.65	1.96
CS5	12.30±0.02	0.53	-0.41	244±8	0.83	0.23	562±24	6.85	3.28	576±14	2.99	2.09	1199±45	3.51	2.32	101±3.2	4.31	2.61
CS6	24.70±0.06	1.14	0.60	310±4	1.13	0.58	236±12	3.08	2.03	536±27	2.98	1.98	964±27	3.03	2.01	154±11	7.04	3.22
CS7	16.70±0.01	0.99	0.03	174±14	0.81	-0.26	160±24	2.67	1.47	385±8	2.74	1.50	966±32	3.88	2.01	125±5.4	7.31	2.92
CS8	20.00±0.03	0.85	0.29	258±11	0.86	0.31	511±7	6.10	3.15	578±15	2.94	2.09	806±34	2.32	1.75	92±9	3.84	2.48
CS9	24.60±0.05	1.20	0.59	234±16	0.90	0.17	198±6	2.74	1.78	435±9	2.56	1.68	1006±32	3.35	2.07	19.9±0.1	0.96	0.27
CS10	26.40±0.02	1.18	0.69	194±15	0.90	0.17	120±5	1.51	1.06	548±14	2.94	2.01	19.5±0.1	0.06	-3.62	19.9±0.1	0.88	0.27
Max	26.40			310			562			578			1822			154		
Min	8.25			80			70			155			20			19.5		
SD	5.66			57			148			95			415			34.5		
Mean	17.55			200			296			433			877			79.4		
World normal	7.20			73			200			19			307					
Toxic limit	20.00						100(400)											

4. Result and analysis

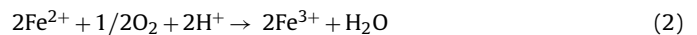
4.1. Soil quality

The agricultural soils that are irrigated by mine drainage water contain very high levels of potentially toxic trace elements, although the total contents vary considerably depending on the location of the samples (Table 1). The pH values range from 6.13 to 8.70 with the mean of 7.25. The values of EC and TOC range from 41 to 210 $\mu\text{S m}^{-1}$ and 6.79 to 64.14 mg/kg with means of 150 $\mu\text{S m}^{-1}$ and 27.02 mg/kg, respectively. The mean concentrations of Ti, Mn, Fe, Zn, As, Rb, Sr, Pb and Zr are 14,427, 1886, 59,853, 296, 17.55, 200, 296, 433 and 877 mg/kg, respectively. Potassium and Ca show the highest concentrations in the range of 10,400–24,400 and 12,600–77,000 mg/kg, respectively, with the mean values in 2–5 orders of the world normal averages (Table 1). Noticeable Zn and Pb concentrations were recorded among all the points in the study area. Arsenic concentration ranges widely from 8.25 to 26.4 mg/kg, with 17.55 mg/kg as the mean value. The Pb, Mn, Zn and As concentrations reported here are likely to be of concern to human health and the environment.

The release of high metal content in the mine drainage soil is dependent on the weathering effects of mine drainage water [23]. Pyrite weathering releases soluble ferrous iron (Fe^{2+}) and acidity that is represented by production of protons (Eq. (1)):



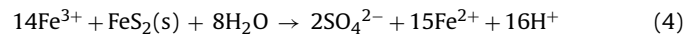
If sufficient dissolved oxygen is present or solutions can be oxygenated by contact with the atmosphere, the dissolved ferrous iron will be oxidized to ferric iron (Fe^{3+}), consuming acidity in the process (Eq. (2)):



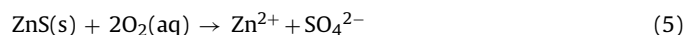
When ferric iron reacts further to precipitate as iron oxyhydroxide minerals, a much greater net production of acidity occurs (Eq. (3)):



This may react with pyrite to produce more acidity and ferrous iron (Eq. (4)):



Mine water often attains solubility equilibrium with these minerals because the forward and reverse reactions are relatively rapid for the precipitation and dissolution of ferric hydroxide compared to residence times of discharge water in mine workings [23]. The ferrous iron produced by the earlier reaction can be re-oxidized by available dissolved oxygen, perpetuating the cycle represented by the reactions (Eqs. (2)–(4)). Metal sulfides other than pyrite will not necessarily produce acidity, but will release soluble metal ions to solution. For example, sphalerite (ZnS) will release Zn into the environment by oxidization through the reaction below (Eq. (5)):



Similarly, Mn, Ti, Pb, As, Sr and Zr are released from siderite, rutile and anatase, galena, melnikovite and mispickel, strontianite and zircon, respectively [24,25].

Although kaolinite commonly contains anatase and rutile as impurities, Ti may also substitute for Al in tetrahedral sites [26]. Kaolinite decomposition during the carbonization process would then be expected to release TiO_2 . This suggests that kaolinite is the main source of the TiO_2 . Average claystones and siltstones are normally enriched in Rb [27]. It is generally thought that these two elements have mainly aluminosilicate affinity [28].

Lead is generally associated with mineral matter in coal, primarily with sulfides such as galena (PbS), clausthalite (PbSe) [24] and

Table 2
Metal contamination factors (CFs) and pollution load indices (PLIs) for agricultural soil.

Sample	Contamination factors (CFs)											PLI	
	K	Ca	Ti	Mn	Fe	Zn	As	Rb	Sr	Pb	Zr		Nb
ES1	2.20	23.69	2.90	4.32	1.48	5.66	0.76	1.31	10.60	5.41	7.19	6.36	2.72
ES2	2.10	8.83	2.15	4.29	1.31	3.94	0.99	0.87	6.65	5.76	3.58	6.09	2.63
ES3	2.52	5.23	2.52	2.51	1.26	3.38	1.31	1.31	6.68	3.81	10.12	10.91	2.21
ES4	2.08	5.08	2.24	3.78	1.05	6.84	1.62	0.58	8.18	4.12	3.29	5.00	2.83
ES5	2.44	3.88	3.72	3.19	2.05	5.59	0.86	1.55	14.42	5.20	6.87	8.64	2.77
ES6	4.29	16.06	2.72	2.81	2.25	1.99	2.00	2.22	3.82	4.93	6.14	4.91	2.62
ES7	4.49	13.17	2.48	2.34	1.21	2.22	1.20	1.12	1.82	1.71	5.16	2.27	1.67
ES8	2.30	10.09	3.42	6.14	2.09	7.10	2.09	1.72	13.01	5.50	5.52	7.27	4.02
ES9	2.28	7.02	2.19	3.15	2.06	2.52	2.24	1.69	2.55	3.66	0.12	1.81	2.66
ES10	2.44	6.40	2.38	3.61	1.80	2.21	1.77	1.33	4.88	4.22	4.26	6.36	2.54
WS1	3.27	20.55	3.10	4.08	1.36	6.42	0.89	1.52	9.56	4.92	7.75	7.00	2.75
WS2	4.23	8.03	2.54	4.11	1.45	4.21	1.16	0.71	7.95	5.73	3.96	8.73	2.78
WS3	3.03	4.92	2.13	2.89	1.34	4.31	1.21	1.61	7.19	3.92	7.66	9.45	2.40
WS4	2.68	5.26	2.48	4.15	1.13	7.02	1.84	0.69	10.78	4.67	3.48	10.45	3.09
WS5	3.05	4.06	3.52	3.09	2.02	6.20	1.77	1.54	11.82	4.87	6.89	8.27	3.20
WS6	4.09	15.26	2.68	2.83	2.10	3.69	2.04	2.09	4.13	4.49	6.28	7.73	2.89
WS7	3.89	15.02	3.10	2.32	1.31	2.38	1.30	1.23	4.23	2.93	6.16	11.36	1.94
WS8	3.31	9.17	3.60	5.61	2.15	7.25	1.99	1.75	12.42	5.66	4.83	8.00	3.97
WS9	4.51	7.26	2.36	3.56	2.00	3.33	2.43	1.62	5.14	4.11	0.12	1.81	2.98
WS10	4.35	5.54	2.17	3.94	2.11	3.02	2.03	1.40	2.81	5.17	7.01	6.09	3.05
CS1	4.03	16.74	3.50	4.50	1.83	6.67	0.93	1.39	12.99	5.19	7.70	7.91	3.05
CS2	3.91	14.68	2.32	4.37	1.90	4.71	1.01	1.18	8.21	5.88	4.21	8.73	2.97
CS3	4.33	6.52	3.52	2.80	1.17	4.31	1.48	1.39	6.44	3.70	11.39	9.00	2.38
CS4	3.69	6.00	2.60	3.59	1.60	5.49	2.06	1.24	8.08	4.22	3.83	5.82	3.07
CS5	3.45	11.26	3.91	2.96	2.13	6.51	1.13	1.76	14.60	6.36	7.49	9.18	3.12
CS6	4.09	14.52	3.12	2.73	1.99	3.36	2.27	2.24	6.13	5.92	6.03	14.00	3.01
CS7	4.29	12.55	3.06	2.56	1.56	2.85	1.54	1.26	4.16	4.25	6.04	11.36	2.36
CS8	3.91	16.12	3.56	6.33	2.18	6.48	1.84	1.86	13.27	6.39	5.04	8.36	4.02
CS9	4.23	10.71	2.21	3.58	1.88	3.77	2.26	1.69	5.14	4.81	6.29	1.81	3.08
CS10	4.89	5.78	3.79	3.93	2.06	3.60	2.43	1.40	3.12	6.06	0.12	1.81	3.36

pyrite, as well as aluminosilicates and carbonates [29]. Swaine [30] suggests that an organic association may be possible for containing Pb, most likely in the lower rank coals.

4.2. Indices of pollution

The results of the present study show that with the exception of Rb, most of the metals are significantly enriched in the agricultural soils (Table 1). The EF values for Ti range from 1.1 to 3.71, Mn from 1.25 to 3.67, Zn from 0.88 to 6.53, As from 0.42 to 1.63, Rb from 0.34 to 1.2, Sr from 1.24 to 7.81, Pb from 1.42 to 4.40, Zr from 0.06 to 4.86 and Nb from 0.88 to 8.69. Overall, the average order of EF values for the metals is Sr (4.63) > Nb (4.49) > Zr (3.43) > Pb (2.84) > Zn (2.80) > Mn (2.20) > Ti (1.72) > As (0.95). The highest EFs (1.55 and 1.63) for As occur at points ES4 and WS4, which are located linearly at the same distance from the mine site. According to Zhang and Liu [31], EF values between 0.05 and 1.5 indicate that the metal is entirely from crustal materials or natural processes, whereas EF values higher than 1.5 suggest that the sources are more likely to be anthropogenic. Han et al. [32] divide the contamination into different categories based on EF values, where $EF \leq 2$ suggests deficiency to minimal metal enrichment, whereas $EF > 2$ suggests several degrees of metal enrichment.

The geoaccumulation index (I_{geo}) introduced by Muller [21] was also used as a reference of estimating the extent of metal pollution. The I_{geo} values for the metals of environmental interest are 0.52–1.38 for Ti, 0.63–2.08 for Mn, 0.41–2.27 for Zn, 0.42–1.63 for As, –1.37–0.58 for Rb, 0.28–3.28 for Sr, 0.19–2.09 for Pb, –3.62–2.92 for Zr and 0.27–3.22 for Nb (Table 1). The I_{geo} values indicate moderate to heavily pollution of investigated metals in the study area, although some deviation is observed depending on each metal and sampling location. Among the environmentally most toxic metals, Mn, Zn and Pb are significantly accumulated in the soils, as indicated by their respective average I_{geo} values of 1.24 ± 0.38 , 1.49 ± 0.58 and 1.63 ± 0.38 . In contrast, the I_{geo} value of

Rb (-0.122 ± 0.47) is less than zero, suggesting that the area is not polluted by this metal. Among the 10 sampling sites, the I_{geo} value of Pb is slightly higher in the drained soils than the bank soils. The contamination factors (CFs) of the heavy metals of environmental concern range as Ti: 2–3.7, Mn: 3–6.5, Zn: 2–6.5, Sr: 1.8–14.6, Pb: 1.71–6.39, Zr: 0.12–10.12, Fe: 1–2 and As: 0.76–2.43 (Table 2). The pollution load index (PLI) calculated from CF shows that the soils are moderately to heavily contaminated by investigated heavy metals (Table 2). The sampling Site 8 shows the highest PLI (4.02) within the study area and Sites 4, 5 and 10 are second highest (PLI around 3) and the rest of the area is low to moderately polluted.

4.3. Pollution source identification

For further evaluation of extent of metal contamination in the study area and source identification, principal component analysis was used following standard procedure reported in literature [12,33–36]. PCA was performed on the logarithmic form of the metal data. Varimax rotation [37] was used to maximize the sum of the variance of the factor coefficients. This technique clusters variables into groups, such that variables belonging to one group are highly correlated with one another. The results of the PCA of heavy metal contents are shown in Table 3. Five principal components (PCs) with eigenvalues greater than 1 were extracted. PCA leads to a reduction of the initial dimension of the dataset to five components which explain 80% of the data variation. Therefore, these five factors play a significant role in explaining metal contamination in the study area.

In details, principal component 1 (PC1), which has the highest loadings of Mn, Pb, Sr, Zn and accounts for 21% of variance (Table 3), and is the most important component. PC1 could be better explained as anthropogenic source, specifically derived from coal mine effluents. Zinc, Sr and Pb may be released from sphalerite, strontianite, goyazite, galena and clausthalite minerals that are associated with coal seams. Studies elsewhere have also reported

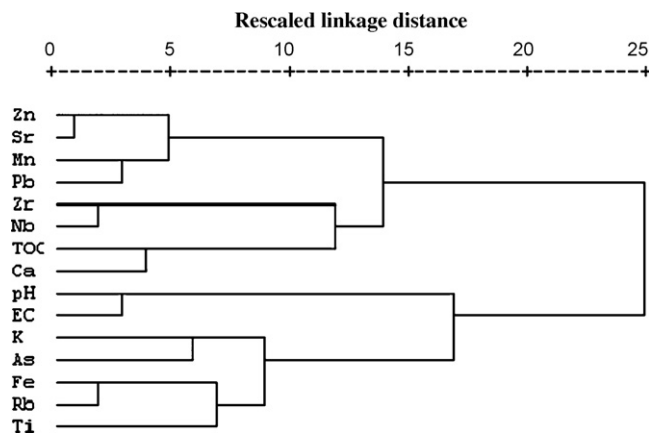
Table 3

Rotated component matrix of five-factor model with moderate to strong loadings in bold typeface.

Parameter	PC1	PC2	PC3	PC4	PC5
pH	-0.035	-0.150	-0.066	0.808	-0.101
EC	-0.106	0.033	-0.005	0.940	0.011
TOC	0.328	0.017	-0.042	-0.049	0.889
As	-0.110	-0.506	0.520	0.332	-0.279
Ca	-0.101	0.111	0.152	-0.580	0.586
Fe	0.219	-0.231	0.868	-0.112	-0.046
K	-0.410	-0.110	0.464	-0.090	0.478
Mn	0.852	-0.256	0.004	-0.093	0.144
Nb	0.174	0.884	-0.002	-0.055	-0.131
Pb	0.744	0.039	0.368	-0.374	-0.133
Rb	-0.122	0.060	0.866	-0.099	0.094
Sr	0.818	0.499	-0.010	-0.005	0.046
Ti	0.329	0.410	0.512	0.091	0.329
Zn	0.864	0.276	-0.102	0.102	0.165
Zr	-0.016	0.860	-0.094	-0.089	0.104
Eigenvalues	3.207	2.442	2.433	2.194	1.666
% of variance	21.377	16.280	16.223	14.624	11.106
Cumulative %	21.377	37.657	53.880	68.505	79.610

on similar observations [24,25]. The significant source of Mn is Mn-rich siderite that is common in fresh- to brackish-water sub-aqueous sediments that overlie coal. According to Larsen and Mann [38], this is especially the case for coals formed in wet, tropical environments. Manganese, Pb, Sr, Zn have close association with organic matter [39]. Geochemical weathering of sulfide minerals derived from mine drainage contributes to enrichment of the soil with these heavy metals. Considering the above reasons, the components loading of PC1 may have been derived from coal mine drainage sources, and PC1 may be defined as a coal mine drainage component. PC2, which has high positive loadings of Nb and Zr, moderate positive loading of Sr and negative loading of As, accounts for 16% of variance. PC2 can be considered as a measure of leaching of crustal materials because an important fraction of all the metals is lithogenic. Strontium is highly correlated with PC1 and moderately correlated with PC2, indicating a mixed source from both lithogenic and anthropogenic inputs. PC3 has high loadings of As, Fe, Rb and Ti and accounts for 16% of variance. PC3 can be considered as an atmospheric component. Coal mine dust and fly ash (derived from the nearby thermal power plant) consist of some sulfide mineral particles which are deposited in the vicinity of the mine. The sulfide minerals (e.g. pyrite, melnikovite, mispickel etc.) may be oxidized in an open environment and release As and iron oxides to soil. The oxide minerals, such as rutile, anatase and brookite, often associated with coal and deposited as mine dust also react in acid mine drainage and release Ti to the soil. PC4, which is highly loaded with pH and EC and negatively loaded with Ca, accounts for 15% of variance and can be considered as the agriculture factor. For irrigation purposes, the farmers often use the mine drainage water and chemical fertilizer that often release some ion in soil. PC5, which accounts for 11% of the total variance, is characterized by high loadings of TOC, Ca and K, and can be explained by the significant role of organic matter that is bound closely with Ca and K.

Based on information assessed from principal component analysis, hierarchical cluster analysis was performed [37]. Four main clusters can be distinguished in the dendrogram obtained from the CA performed on the analyzed parameters with Ward's method and the squared Euclidean distance as a similarity measure (Fig. 2). Cluster 1 includes elements Zn, Sr, Mn and Pb, which in the previous section were identified as contaminants derived from anthropogenic sources (coal mine drainage). Cluster 2, which contains Zr, Nb, TOC and Ca, are derived from organic matter and chemical weathering of some metal bearing minerals. Cluster 3 contains pH and EC derived from agricultural activities, which is mostly controlled by anthropogenic sources. Cluster 4 contains K, As, Fe,

**Fig. 2.** Dendrogram obtained by hierarchical clustering analysis for parameters.

Rb and Ti which support the factor scores are mainly generated from mine dust and coal fly ash that are controlled by atmospheric processes.

Similarly, sampling points were also analyzed by clustering methods (Table 4) and organized in the dendrogram to identify the identical geochemical groups (Fig. 3). The sampling points WS8, ES8, CS8, WS5, ES5, CE5, ES1, CS1 and WS1 are clustered in Group 1. Group 2 contains WS2, ES2, WS4 and ES4. The sampling points WS9, ES9 and CS10 are included in Group 3, whereas Group 4 contains ES6, CS6, WS6, WS10, ES10, CS9, ES7, CS7, WS3, ES3, CS3, CS4 and WS7. Sites 1, 5 and 8 belong to Group 1 and are highly loaded with Zn, Sr, Mn and Pb. Group 2 includes Sites 2 and 4, which are loaded with Zr, Nb, TOC and Ca. Group 4 consists of Sites 3, 6, 7 and 10 which are enriched with K, As, Fe, Rb and Ti. Among all the sites, the sites of Groups 1 and 4 are the most polluted in the study area and dominantly controlled by anthropogenic activities, especially from Barapukuria coal mining and coal fired thermal power plant.

Table 4

Scores for the five-factor model for sampling sites with relatively high scores in bold typeface.

	PC1	PC2	PC3	PC4	PC5
WS1	0.88416	0.17451	-1.16319	-1.95265	0.99428
WS2	0.53523	-0.36836	-1.71273	-1.53221	-1.28093
WS3	-0.74539	1.13468	-0.67940	0.78145	-1.13714
WS4	0.79205	-0.46018	-2.28574	1.30821	-0.87642
WS5	0.81792	1.21475	0.31632	0.98141	-0.60810
WS6	-1.44269	-0.02983	1.49642	-2.49383	-1.62475
WS7	-2.62835	-0.43741	-1.24946	0.82993	1.66638
WS8	1.70352	-0.02602	0.69268	0.70423	-0.11836
WS9	-0.55717	-2.35176	0.09905	0.42723	-0.97464
WS10	-0.42646	-0.23468	-0.12392	0.36415	-1.12649
ES1	0.44942	0.50599	-0.62893	-1.15669	1.37737
ES2	0.35769	-0.10604	-1.07790	-1.16257	-0.26855
ES3	-0.51029	0.75392	-0.58986	0.22975	-1.01571
ES4	0.85590	0.17714	-1.47760	0.25479	-1.13513
ES5	0.47571	0.94607	0.87005	0.74351	-1.27673
ES6	-0.95343	0.32731	1.19156	-0.80068	-0.32205
ES7	-1.76605	1.05819	-0.30056	0.57395	0.62120
ES8	1.46006	0.07077	1.02023	0.78791	0.27632
ES9	-0.14598	-2.36624	0.48701	0.65296	0.36137
ES10	-0.45241	-0.57211	0.51939	0.56897	-0.57548
CS1	0.83869	0.51468	-0.04192	-1.13516	1.74665
CS2	0.52135	-0.16689	-0.45272	-1.24694	0.91733
CS3	-0.67652	1.04493	-0.21895	0.71638	1.17016
CS4	0.19532	-0.15928	-0.11151	0.64706	-0.00575
CS5	0.61755	1.27367	1.06089	0.12355	0.31556
CS6	-0.62244	0.86024	1.62294	-0.85958	-0.57264
CS7	-1.09737	0.71512	0.18735	0.82526	0.88970
CS8	1.47450	0.04680	1.22308	0.92084	1.08780
CS9	-0.24359	-1.21853	0.28970	0.13675	1.27737
CS10	0.28909	-2.32146	1.03772	-0.23801	0.21739

Table 5

Pearson correlation matrix for heavy metal in soil samples.

Parameter	Ti	Mn	Fe	Zn	As	Rb	Sr	Pb	Zr	Nb
Ti	1									
Mn	0.203	1								
Fe	0.352	0.278	1							
Zn	0.449*	0.633**	0.001	1						
As	-0.083	0.074	0.478**	-0.214	1					
Rb	0.338	-0.04	0.738**	-0.133	0.402*	1				
Sr	0.575**	0.546**	0.145	0.889**	-0.368*	0.016	1			
Pb	0.397*	0.601**	0.527**	0.469**	0.02	0.223	0.540**	1		
Zr	0.272	-0.23	-0.21	0.126	-0.479**	0.185	0.261	-0.075	1	
Nb	0.299	-0.1	-0.179	0.205	-0.340	0.028	0.364*	0.186	0.545**	1

* Correlation is significant at the 0.05 level.

** Correlation is significant at the 0.01 level.

4.4. Correlation matrix (CM)

Inter-element relationships in soil matrix provide information on heavy metal sources and pathways in the geoenvironment [34]. In general, correlations between metals agreed with the results obtained by PCA, and CM was useful to confirm some new associations between metals that were not clearly stated in previous analysis. According to the values of Pearson correlation coefficients (Table 5), a significant positive correlation ($p < 0.01$) exists between Fe vs. As ($r = 0.478$, $p < 0.01$), Rb ($r = 0.738$, $p < 0.01$), Pb ($r = 0.527$, $p < 0.01$), and Mn shows relatively weak positive correlation with Fe ($r = 0.278$). Titanium (Ti) is significantly correlated with Zn ($r = 0.449$, $p < 0.01$), Sr ($r = 0.575$, $p < 0.01$) and Pb ($r = 0.397$, $p < 0.05$). The strong correlation among elements indicates their common origin, especially from carbonate and sulfide minerals (e.g. sphalerite, strontianite, galena etc.) that are associated with coal seams [24,25]. The significantly positive correlation of As, Pb, Mn and Zn, Ti with Fe indicates that the elements were derived from similar sources and also moving together, especially from coal-bearing minerals in underground mining activities. Zhang et al. [40] also reported similar results for source identification of soil inor-

ganic pollutants in China. No significant correlation between soil pH and heavy metal content was observed for the analyzed soils. These results are consistent with those obtained by Tume et al. [41] for natural surface soils of Catalonia, Spain, characterized by a similar range of pH values and also by Manta et al. [42] for non-stratified soils from Sicily. EC shows negative correlation with metals except Zn and As, similar to the results reported from Dragović et al. [34] in the study of heavy metals in soils. TOC shows strong positive correlations with Ca ($r = 0.458$, $p < 0.05$), Mn ($r = 0.377$, $p < 0.05$) and Zn ($r = 0.396$, $p < 0.05$). The correlations between heavy metal concentrations and soil organic matter content obtained in this study agreed with those of Lee et al. [43] who indicated that soil organic matter content played a fundamental role in the control of Pb sorption by soils. The adsorption of Mn was found to increase with higher soil organic matter content [44], and in previous section described as Mn-rich siderite minerals. X-ray absorption spectrometry and electro spin resonance studies have shown that Pb and Zn form inner-sphere complexes with soil organic matter, i.e. humic acids [45]. Zinc is known to have a high affinity for clays and sesquioxide surfaces [46].

5. Conclusion

Different useful tools, methods and indices have been employed for evaluation of soil pollution in the agricultural soils surrounding the coal mine area in the northern part of Bangladesh. Analysis of soil samples from 30 sampling points in the irrigated field and channel bottom show significant spatial variation of heavy metals (Ti, As, Mn, Zn, Sr, Pb, Rb and Sr). The metal enrichment factor (EF) and geoaccumulation index (I_{geo}) of most of the metals (Ti, Mn, Sr, Zr, Pb and Nb) show that the soils in the study area are moderate to highly polluted, whereas As and Rb are generally within the background levels. Pollution load indices (PLIs) derived from contamination factors show that all sampling points in the study area exceed unity and may be considered as highly polluted sites. Of all the sampling points in the study area, ES8 and WS8, which are located at the distal part of the mine influenced area, show the highest PLI (4.02). Multivariate analysis (PCA, CA) and correlation matrix used in this study provide important tools for better understanding of the source identification and dynamics of pollutants. The PCA applied on the investigated heavy metals identified five components. Among them, PC1 and PC3, which are loaded with Mn, Pb, Sr, Zn, As, Fe and Rb are related to the anthropogenic sources. The same grouping was obtained from cluster analysis. Four main clusters of elements are obtained by CA. The first, third and fourth clusters are considered as anthropogenic sources which are loaded with Zn, Sr, Mn, Pb, pH, EC, K, As, Fe, Rb and Ti. The CA classified all the sampling points into four main groups of spatial similarities, where different sampling points are included in different groups. A significant positive correlation is observed among Sr, Fe, Rb, Pb, Mn,

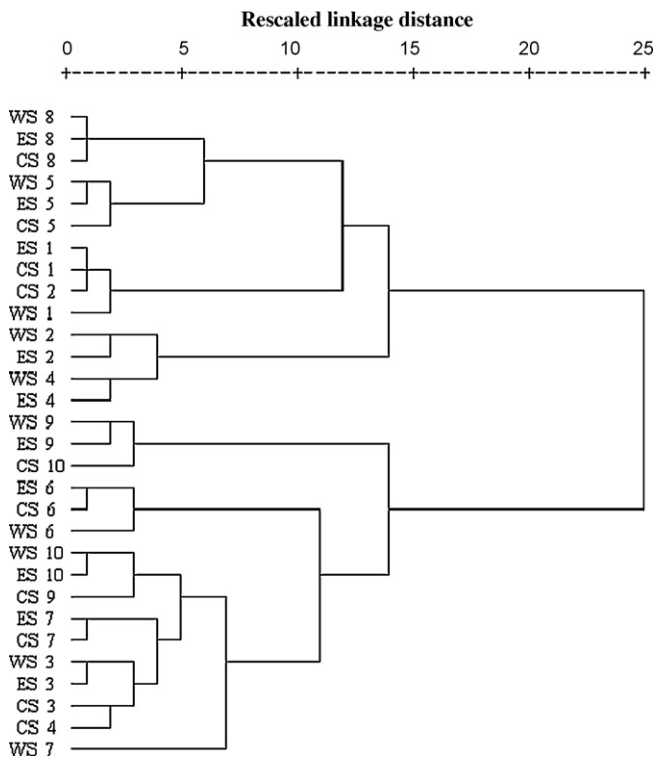


Fig. 3. Tree diagram obtained by clustering of sampling sites.

Ti, Zn and As, indicating that these metals have similar geochemical behavior.

Acknowledgments

The authors are grateful to the Authority of Atomic Energy Center, Dhaka, Bangladesh for providing laboratory facilities for elemental analysis. The first author acknowledges financial support from the Japanese Government (MONBUKAGAKUSHO Scholarship). The authors are grateful to the anonymous reviewers whose critical comments have greatly improved the manuscript.

References

- [1] F. Zhao, Z. Cong, H. Sun, D. Ren, The geochemistry of rare earth elements (REE) in acid mine drainage from the Sitai coal mine, Shanxi Province, North China, *Int. J. Coal Geol.* 70 (2007) 184–192.
- [2] L.S. Tabakslat, Specific features in the formation of the minewater microelement composition during ore mining, *Water Res.* 29 (2002) 333–345.
- [3] D.S. Cherry, R.J. Currie, D.J. Souek, H.A. Latimer, G.C. Trent, An integrative assessment of a watershed impacted by abandoned mined land discharges, *Environ. Pollut.* 111 (2001) 377–388.
- [4] D.C. Adriano, Trace Elements in Terrestrial Environments—Biogeochemistry, Bioavailability and Risks of Metals, Springer, New York, 2001.
- [5] P. Madejón, J.M. Murillo, T. Maranon, F.R. Cabrera, R. Lopez, Bioaccumulation of As, Cd, Cu, Fe and Pb in wild grasses affected by the Aznalcollar mine spill (SW Spain), *Sci. Total Environ.* 290 (2002) 105–120.
- [6] M.H. Wong, Ecological restoration of mine degraded soils, with emphasis on metal contaminated soils, *Chemosphere* 50 (2003) 775–780.
- [7] G.R. MacFarlane, M.D. Burchett, Cellular distribution of Cu, Pb, and Zn in the Grey Mangrove *Avicennia marina* (Forsk.), *Vierh. Aquat. Bot.* 68 (2000) 45–59.
- [8] Z.D. Liu, X.G. Yu, H.B. Xie, Analysis on the course of economic development around the Yangtze River basin in 1990s, *Resour. Environ. Yangtze Basin* 11 (2002) 494–499.
- [9] G.F. Knoll, Radiation Detection and Measurement, John Wiley and Sons, New York, 1971 (reprint of IUPAC document, *Spectrochim. Acta.* 33 (1978) 241).
- [10] P.V. Espen, H. Nullens, F. Adams, A computer analysis of X-ray fluorescence spectra, *Nucl. Instrum. Methods* 142 (1977) 243–250.
- [11] S.R. Taylor, Abundance of chemical elements in the continental crust: a new table, *Geochim. Cosmochim. Acta* 28 (1964) 1273–1285.
- [12] B. Rubio, M.A. Nombela, F. Vilas, Geochemistry of major and trace elements in sediments of the Ria de Vigo (NW Spain): an assessment of metal pollution, *Marine Poll. Bull.* 11 (2000) 968–980.
- [13] D.Z. Jiang, E.J. Teng, Y.L. Liu, The contribution of difference on the element background values in soils and the analysis of variance of single factor on soil groups, *Environ. Monit. China* 2 (1996) 21–24.
- [14] P. Blaser, S. Zimmermann, J. Luster, W. Shotyk, Critical examination of trace element enrichments and depletions in soils: As, Cr, Cu, Ni, Pb, and Zn in Swiss forest soils, *Sci. Total Environ.* 249 (2000) 257–280.
- [15] F. Cabrera, L. Clemente, E.D. Barrientos, R. López, J.M. Murillo, Heavy metal pollution of soils affected by the Guadiamar toxic flood, *Sci. Total Environ.* 242 (1999) 117–129.
- [16] J.I. Yaqin, F. Yinchang, W.U. Jianhui, Z. Tan, B. Zhipeng, D. Chiqing, Using geoaccumulation index to study source profiles of soil dust in China, *J. Environ. Sci.* 20 (2008) 571–578.
- [17] P. Zefer, G.P. Glasby, K. Sefer, J. Pempkowiak, R. Kalisz, Heavy-metal pollution in superficial sediments from the southern Baltic Sea off Poland, *J. Environ. Sci. Health* 31A (1996) 2723–2754.
- [18] K.D. Daskalakis, T.P. O'Connor, Normalization and elemental sediment contamination in the Coastal United States, *Environ. Sci. Technol.* 29 (1995) 470–477.
- [19] G. Muller, Schwermetalle in den sediments des Rheins-Veränderungen seit 1971, *Umschan* 79 (1979) 778–783.
- [20] G. Muller, Die Schwermetallbelastung der sedimente des Neckars und seiner Nebenflüsse: eine Bestandsaufnahme, *Chem. Zeitung* 105 (1981) 157–164.
- [21] G. Muller, Index of geoaccumulation in sediments of the Rhine River, *Geojournal* 2 (1969) 108–118.
- [22] J. Usero, A. Garcia, J. Fraidias, Calidad de las aguas y sedimentos del Litoral Andaluz, in: Junta de Andalucía, Consejería del Medio Ambiente, Sevilla, 2000 (Editorial) 164 pp.
- [23] S.A. Banwart, M.E. Malmstrom, Hydrochemical modeling for preliminary assessment of minewater pollution, *J. Geochem. Explor.* 74 (2001) 73–97.
- [24] J. Hower, J.D. Robertson, Clausthalite in coal, *Int. J. Coal Geol.* 53 (2003) 219–225.
- [25] R. Sakurovs, D. French, M. Grigore, Quantification of mineral matter in commercial coles and their parent coals, *Int. J. Coal Geol.* 72 (2007) 81–88.
- [26] W.A. Deer, R.A. Howie, J. Zussman, Sheet Silicates, Longmans Green and Co. Ltd., London, UK, 1962.
- [27] P.W. Fralick, B.I. Kronberg, Geochemical discrimination of clastic sedimentary rock sources, *Sediment. Geol.* 113 (1997) 111–124.
- [28] F. Goodarzi, Elemental distribution in coal seams at the fording coal mine, British Columbia, Canada, *Chem. Geol.* 68 (1988) 129–154.
- [29] J. Wang, A. Sharma, A. Tomita, Determination of the modes of occurrence of trace elements in coal by leaching coal and coal ashes, *Energy Fuels* 17 (2003) 29–37.
- [30] D.J. Swaine, Trace Elements in Coal, Butterworths, London, 1990, 290 pp.
- [31] J. Zhang, C.L. Liu, Riverine composition and estuarine geochemistry of particulate metals in China—weathering features, anthropogenic impact and chemical fluxes, *Estuar. Coastal Shelf Sci.* 54 (2002) 1051–1070.
- [32] Y.M. Han, P.X. Du, J.J. Cao, E.S. Posmentier, Multivariate analysis of heavy metal contamination in urban dust of Xi'an, Central China, *Sci. Total Environ.* 355 (2006) 176–186.
- [33] I.T. Jolliffe, Principal Component Analysis, Springer, New York, 1986.
- [34] S. Dragović, N. Mihailović, B. Gajić, Heavy metals in soils: distribution, relationship with soil characteristics and radionuclides and multivariate assessment of contamination sources, *Chemosphere* 72 (2008) 491–549.
- [35] L. Yu, G. Xin, W. Gang, Q. Zhang, Q. Su, G. Xiao, Heavy metal contamination and source in arid agricultural soil in central Gansu Province, China, *J. Environ. Sci.* 20 (2008) 607–612.
- [36] A. Franco-Uría, C. López-Mateo, E. Roca, M.L. Fernández-Marcos, Source identification of heavy metals in pastureland by multivariate analysis in NW Spain, *J. Hazard. Mater.* 165 (2009) 1008–1015.
- [37] N.J. Gotelli, A.M. Ellison, A Primer of Ecological Statistics, first ed., Sinauer Associates, Sunderland, MA, USA, 2004, 492 pp.
- [38] D. Larsen, R. Mann, Origin of high manganese concentrations in coal mine drainage, eastern Tennessee, *J. Geochem. Explor.* 86 (2005) 143–163.
- [39] W. Zhang, H. Feng, J. Chang, J. Qu, H. Xie, L. Yu, Heavy metal contamination in surface sediments of Yangtze River intertidal zone: an assessment from different indexes, *Environ. Pollut.* 157 (2009) 1533–1543.
- [40] C. Zhang, L. Wu, Y. Luo, H. Zhang, P. Christie, Identifying sources of soil inorganic pollutants on a regional scale using a multivariate statistical approach: role of pollutant migration and soil physicochemical properties, *Environ. Pollut.* 151 (2008) 470–476.
- [41] P. Tume, J. Bech, L. Longan, L. Tume, F. Reverter, B. Sepulveda, Trace elements in natural surface soils in Sant Climent (Catalonia, Spain), *Ecol. Eng.* 27 (2006) 145–152.
- [42] D.S. Manta, M. Angelone, A. Bellanca, R. Neri, M. Sprovieri, Heavy metals in urban soils: a case study from the city of Palermo (Sicily), Italy, *Sci. Total Environ.* 30 (2002) 229–243.
- [43] S.Z. Lee, L. Chang, H.H. Yang, C.M. Chen, M.C. Liu, Adsorption characteristics of lead onto soils, *J. Hazard. Mater.* 63 (1998) 37–49.
- [44] H.B. Bradl, Adsorption of heavy metal ions on soils and soils constituents, *J. Colloid Interf. Sci.* 277 (2004) 1–18.
- [45] L.J. Lund, E.E. Betty, A.L. Page, R.A. Elliot, Occurrence of high Cd levels in soil and its accumulation by vegetation, *J. Environ. Qual.* 10 (1981) 551–556.
- [46] W.L. Lindsay, Chemical Equilibria in Soils, Wiley and Sons, New York, United States, 1979.